HAL open science

Bidirectional seiching in a rectangular, open channel, lateral cavity

Emmanuel Mignot, Mathilde Pozet, Nicolas Riviere, Simon Chesne

To cite this version:

Emmanuel Mignot, Mathilde Pozet, Nicolas Riviere, Simon Chesne. Bidirectional seiching in a rectangular, open channel, lateral cavity. CFM 2015 - 22ème Congrès Français de Mécanique, Aug 2015, Lyon, France. hal-03444767

HAL Id: hal-03444767

https://hal.science/hal-03444767v1

Submitted on 23 Nov 2021

HAL is a multi-disciplinary open access archive for the deposit and dissemination of scientific research documents, whether they are published or not. The documents may come from teaching and research institutions in France or abroad, or from public or private research centers.

L'archive ouverte pluridisciplinaire **HAL**, est destinée au dépôt et à la diffusion de documents scientifiques de niveau recherche, publiés ou non, émanant des établissements d'enseignement et de recherche français ou étrangers, des laboratoires publics ou privés.

Bidirectional seiching in a rectangular, open channel, lateral cavity

E. MIGNOT[a], M. POZET[a], N. RIVIERE[a], S. CHESNE[b]

a. Université de Lyon, LMFA, INSA, Bat. Jacquard, 20 av. A. Einstein, 69621 Villeurbanne, France – emmanuel.mignot@insa-lyon.fr
b. Université de Lyon, CNRS INSA-Lyon, LaMCoS UMR5259, F-69621, Villeurbanne, France

Résumé :

Le travail présenté ici s'intéresse aux oscillations de surface libre de cavités latérales, c'est à dire des cavités horizontales à surface libre connectées sur un de leur côté à un écoulement permanent. Ce phénomène d'oscillation, appelé Seiching, est étudié expérimentalement, tout d'abord pour une cavité carrée, puis pour une cavité rectangulaire. Les oscillations de surface libre sont mesurées et, pour la cavité carrée, deux ondes stationnaires coexistantes apparaissent et sont chacune reconstruites en utilisant des méthodes d'analyse de signal. De plus, il apparaît que les fréquences d'oscillation correspondantes sont en bon accord avec les pics de fréquence du spectre de vitesse mesuré dans la couche de mélange. Finalement, pour la cavité rectangulaire l'onde stationnaire d'axe perpendiculaire à l'écoulement principal disparaît et une nouvelle onde d'axe longitudinal apparait dans la cavité.

Abstract :

The present work is dedicated to the free-surface oscillation of lateral cavities, i.e. horizontal cavities with free surface connected along one of their sides to a steady main flow. This oscillation phenomenon, named seiching, is studied experimentally, first for a square cavity and then for a rectangular one. Water surface oscillations are recorded and, for the square cavity, two standing waves of perpendicular axes appear to co-exist and are reconstructed individually using usual signal processing tools. Moreover, the corresponding oscillation frequencies appear to be well correlated with the peak frequencies of the velocity spectrum in the mixing layer. Finally, for the rectangular cavity, the standing wave of axis perpendicular to the mainstream axis disappears and an additional standing wave of streamwise axis appears.

Mots clefs : Seiching; free-surface oscillation; lateral cavity; mixing layer; peak frequency

1 Introduction and theoretical background

Present work is dedicated to open-channel lateral cavities, *i.e.* horizontal cavities with free surface connected along one of their sides to a main free-surface flow. Such cavities are encountered in various natural (oxbows, cut-off meanders) or artificial (harbors connected to a river) open-channel hydrodynamic situations.

1.1 Flow pattern in the cavity

The flow in the mainstream is permanent while the cavity is initially at rest. Nevertheless, the transfer of momentum from the mainstream towards the cavity creates a flow in the cavity: one or several recirculation cells occurs in the cavity depending on the width to length aspect ratio of the cavity (see Riviere *et al.*, 2010). For a square cavity where the width (W) and length (L) of the cavity (see Fig.2) are equal, several authors reveal that a single horizontal cell occupies most of the available space in the cavity, with a typical velocity about 1/8 of the main stream cavity (see Cai *et al.*, 2014). This strong velocity gradient between the main stream and the cavity leads to a mixing layer aligned along the interface between the two regions, that is along the segment joining the upstream and downstream corners of the cavity (see Fig.2).

1.2 Coherent structures in the mixing layer

As expressed by several authors in simple mixing layers (Loucks and Wallace, 2012) or in mixing layers at the interface of an open-channel lateral cavity (Sanjou *et al.*, 2012; Sanjou and Nezu, 2013), coherent turbulent structures (named eddies in the present text) are generated near the upstream corner of the mixing layer and are advected along the mixing layer towards the downstream corner. These eddies cause an alternation of rapid and slow streamwise velocity components. Thus, as when impacting on the downstream corner the kinetic energy of the flow is transferred to potential energy and causes a water depth rise at the stagnatuion point,the streamwise velocity fluctuation at the downstream corner creates a fluctuating local water depth. As a consequence, small waves propagate in all directions, including within the cavity.

1.3 Frequency of the passing eddies

The frequency at which the eddies are created and impact the downstream corner and generate small waves is a function of the geometry of the mixing layer and the velocity gradient across the mixing layer, which is itself a function of the velocity of the recirculation cell in the cavity, itself a function of the momentum transfer from the main stream towards the cavity which depends on the characteristics of the mixing layer. The system is then strongly interdependent, and to our knowledge, no method exist to predict the frequency of the passing eddies .

1.4 Seiching phenomenon

If the natural frequency of the cavity is in agreement with the eddies passing frequency, the oscillation of the free-surface amplifies and the so-called seiching takes place, with free-surface oscillations that can reach 1.5 meter on the field (Refmar, 2014). The natural frequency of a cavity is computed as follows. For a cavity with a simplified rectangular shape, Wüest and Farmer (2003) or Sorensen and Thompson (2006) explain that Merian formula relates the width of the cavity W (or its length L, see Fig.2), the water depth in the cavity h and the possible seiche frequency f_{nat} (equal to the natural frequency of the cavity) as:

$$f_{nat} = \frac{n\sqrt{gh}}{2W} \tag{1}$$

That is the wave length λ_{nat} equals:

$$\lambda_{nat} = \frac{2W}{n} \tag{2}$$

with *n* being an integer.

As a consequence, the seiching phenomenon is likely to occur in the direction perpendicular to the main stream (Eq.3) or parallel to the main stream direction (Eq.4) if the dimensions of the cavity are:

$$W = \frac{n}{2}\lambda \tag{3}$$

or

$$L = \frac{n}{2}\lambda \tag{4}$$

as sketched by Wüest and Farmer (2003, see their Figure.1).

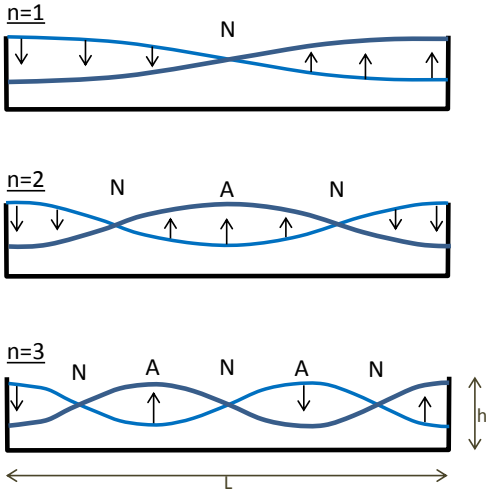

Figure 1: Possible amplified waves in a cavity for n=1, 2 and 3 with N=Nodes and A=Antinodes.

1.5 Summary and scientific purposes

To summarize, the frequency peak in the mixing layer, corresponding to the eddies passing frequency, is a function of the mainstream (mainly mean velocity, water depth and lateral boundary layer development) and of the geometry of the cavity. On the other hand, the natural frequencies of the cavity are functions of its dimensions: length, width, and water depth (see Eqs. 3 &4). If both are similar, the seiching phenomenon occurs and the water volume in the cavity starts to oscillate (as shown on Fig. 1). Nevertheless, such a seiching may affect the characteristics of the mixing layer and thus of its peak frequency (feedback effect, see Tuna *et al.*, 2013). Due to this difficulty that all parameters seem to be linked to each other, the approach selected corresponds to the following steps:

Step 1: establish one experimental flow configuration where seiching appears to occur.

Step 2: measure the characteristics of the oscillation of the cavity volume and reconstruct the corresponding standing waves.

Step 3: measure the velocity components of the mixing layer and estimate its corresponding frequencies.

Step 4: slightly modify one characteristic of the system (here: modify the width *W* of the cavity) and observe the modifications in the mixing layer and cavity oscillations.

2. Experimental set-up

2.1 Description of devices

The experiments are performed in the channel intersection facility at the Laboratoire de Mécanique des Fluides et d'Acoustique at the Université de Lyon. The facility consists of a 4.9 m long horizontal glass channels of rectangular shape sections, *b*=0.3m wide (see Fig.2). A lateral cavity of length L=0.3m is included at the center of the channel, with no step (same bottom elevation) which width *W* can be precisely adjusted. A honeycomb at the inlet of the upstream branch serves to stabilize and straighten the inlet flow (Step 1). Moreover, a sharp crested weir is used to adjust the water depth at the outlet section of the downstream branch. The inlet discharge *Q* is measured using an electromagnetic flowmeter (Promag 50 from Endress Hauser; accuracy ±0.05L/s). The water depth *h* is measured using a digital point gauge at the intersection between the cavity and the mainstream and appears to remain constant in the whole cavity area, at least when no seiching occurs.
The water depths in the cavity (Step 2) are measured using either resistive probes or ultrasonic probes, both permitting a local water depth measurement at frequency higher than 10 Hz, with an uncertainty of about 0.1 mm. The 3 components of the flow velocity in the mixing layer (Step 3) are measured using an ADV (Acoustic Doppler Velocimeter) at a sampling frequency of 50 Hz.

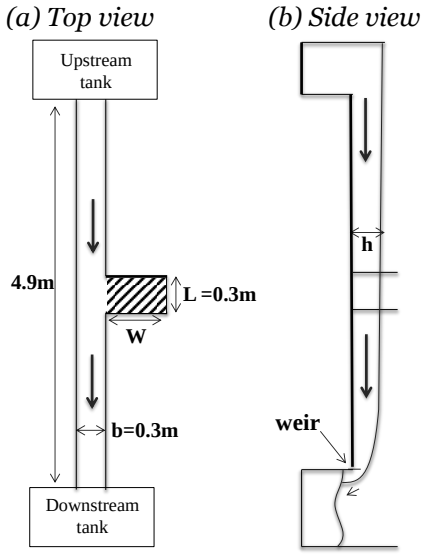

Figure 2: Top and Side view of the experimental set-up.

2.2 Step1: setting a reference configuration

In a first attempt, the cavity is square (*L*=*W*=0.3m). The selection of the reference flow is performed as follows. Tuna *et al.* (2013) showed that if the typical velocity of the mainstream is low, seiching may appear but its amplitude remains too low to be accurately measured using our sensors. For instance for a mainstream bulk velocity of *U*=20 cm/s, equaling the kinetic (U^2/2g) to a potential energy (Δh) leads to a typical amplitude of Δh ~ 2mm for which capillary effects cannot be neglected. We thus decided to select a higher mainstream velocity. The weir is removed (the downstream flow being thus in critical regime) and the mainstream discharge *Q* is regularly increased in order to increase its velocity. Fig.3 confirms that as the mainstream velocity increases the amplitude of the water depth oscillations in the cavity also increases until a mainstream velocity where it decreases again. This is due to the fact that as the mainstream discharge increases, the peak frequency in the mixing layer changes and is thus not not likely to be equal to a natural frequency of the cavity. The mainstream configuration selected

as reference configuration is finally the one within the red circle. The reference configuration is thus L=W=0.3m, U=47cm/s, h=6cm, and the gravity waves celerity $c=\sqrt{gh}=0.77m/s$.

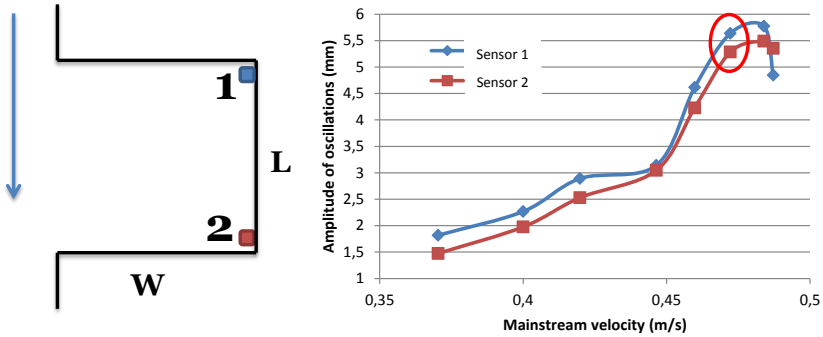

Figure 3: Amplitude of the square cavity oscillation measured at two locations 1 and 2 for an increasing mainstream velocity.

3. Results for the reference configuration

3.1 Step 2: measurement of the water depth oscillation in the cavity

Once the reference configuration is set, a seiching phenomenon is observed and the aim of the present section is to identify all characteristics of the oscillation pattern. To do so, a preliminary work consists of locating a water depth sensor measuring the water depth oscillation during about a minute near the upstream-extremity corner of the cavity as sketched on Fig.4a. The corresponding power spectral density, plotted on Fig.4b reveals two peak frequencies f_1=0.5859Hz and f_2=1.27Hz, which should then correspond to two standing waves. Application of Eq.1 reveals that the natural frequencies of the cavity for the reference configuration are:

- for a length L=0.3m, n=1 (half a wavelength, see Fig.1) leads to $f_{nat\text{-}1}$=1.279Hz quite similar to f_2, corresponding to wave 1 in Fig.4c
- for a length b+W=2W=0.6m, n=2 (one wavelength) leads to $f_{nat\text{-}2}$=1.279Hz, quite similar to f_2 corresponding to wave 2 in Fig.4c.
- for a length b+W=2W=0.6m, n=1 (half a wavelength) leads to $f_{nat\text{-}3}$=0.639Hz quite similar to f_1 corresponding to wave 3 in Fig.4c.

The measured frequency f_2 could then correspond to the waves 1 or 2 sketched on Fig.4c. Indeed waves 1 and 2 present the same wavelength due to particular dimension of the set up ($2L=b+w$). Frequency f_1 seems to correspond to wave 3.

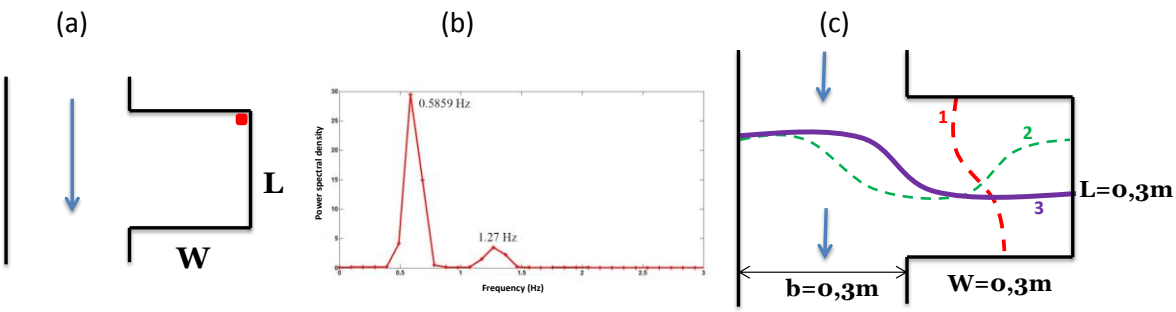

Figure 4: Location of the sensor (a) and corresponding water depth power spectrum (b); possible sketch of the possible standing wave following these results

Detecting which standing wave actually occurs in the reference configuration is not straightforward as the presence of the two waves with different period does not allow a direct estimation. A usual method of signal processing is then applied in order to extract and identify the various waves. One water depth sensor is fixed close to the upstream-extremity corner of the cavity and will be used as a phase reference (referred to as "reference" in Fig.5a) and remains there for the whole measurement duration; a second sensor (referred to as "mobile" in Fig.5a) is located in the cavity or the main stream. The two water depth signals are measured simultaneously during 60 seconds for each configuration (corresponding to one location of the mobile sensor) with a sampling frequency equal to 200 Hz. The measurement grid for the mobile sensor contains 84 measurement points separated by 5cm in both directions. The cross-spectrum of these two signals is used to identify the relative phase of each measurement point in the grid (each location of the mobile sensor) compared to the "reference" sensor (see top of Fig.5c). The corresponding amplitude is estimated through the auto-spectrum of each measurement (see bottom of Fig.5c) where, as expected, f_1 and f_2 are retrieved as peak frequencies.

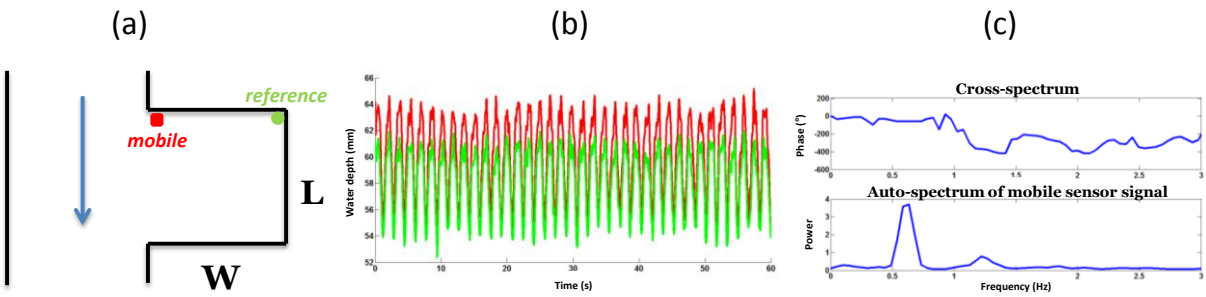

Figure 5: Location of the reference and mobile sensors (a) and corresponding water depth signal (b) and co-spectrum (c) in terms of phase shift (top) and power (bottom).

Once the 84 cross-spectrum along with the 84 auto-spectrum are obtained, the idea is to reconstruct a fictive 2D free-surface for each of the two peak frequencies (f_1 and f_2) at different times during one period of oscillation. For example, for the mobile sensor at one location (as on Fig.5a), for frequency f_1 at time t, the corresponding relative depth h' equals:

$$h'(t) = Ae^{i(\varphi+t)} \tag{5}$$

where A is the square root of the integral of the auto-spectrum of the mobile sensor signal in the frequency range around f_1 and φ is the phase shift between the mobile and reference sensor signals for this same frequency. Once the 84 relative water depths are obtained for this frequency and this time, the free-surface at this time can be reconstructed; the resulting graph is as plotted on Fig.6. In this Figure, plots for both frequencies are given, at two times corresponding to the crest and drought of the reference signal location.

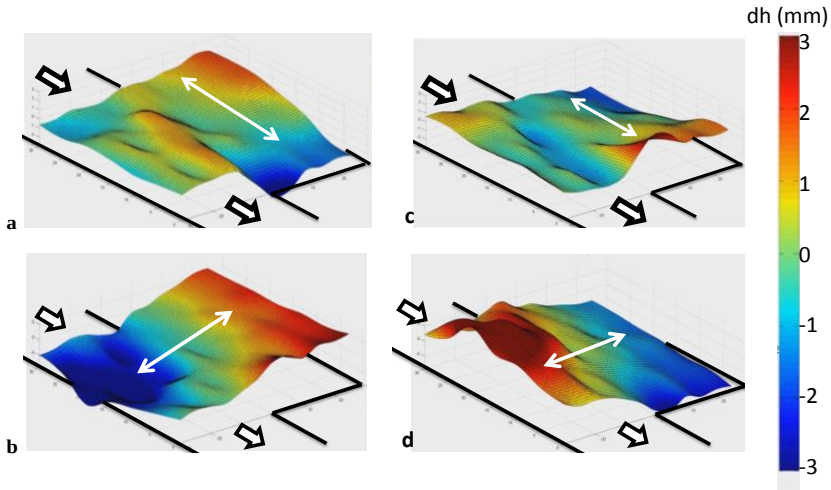

Figure 6: 2D free-surface elevations during the crest (a,b) and drought (c,d) of the free-surface at the reference sensor location for frequencies: f_2=1.27Hz (a,c) & f_1=0.58Hz (b,d). White arrows are added for reading simplicity.

From Fig.6 plots, the two superimposed standing waves can now easily be identified:
- a uninodal standing wave of frequency f_1 (Fig 6b and d), corresponding to the expected wave 3 in Fig. 4c, appears across the cavity and mainstream width with one node at the interface between the mainstream and the cavity and two antinodes, located along the mainstream right side wall and the extreme wall of the cavity.
- a uninodal standing wave of frequency f_2 (Fig. 6a and c) corresponding to wave 1 in Fig.4c, forms in the cavity with one node at the center of the cavity and two antinodes, located along the cavity upstream and downstream walls. This analysis proves that hypothetic wave 2 in fig.4c does not occur.

3.2 Step 3: measurement of the mixing layer spectrum

The aim of the present section is to verify that the water body oscillation frequencies are actually in agreement by the mixing layer peak frequencies. Note that the terminology "be in agreement" was used rather "governs" as it is likely that the cavity oscillation proceeds as a retro-action on the mixing layer and thereby modifies the mixing layer peak frequencies. The mixing layer velocity signal is measured in the mixing layer and the corresponding power spectrum for the transverse velocity component v is given in Fig. 7. Two peaks clearly appear with frequencies equal to f_{1ADV}=0.5859Hz, similar to f_1 and f_{2ADV}=1.196Hz, quite similar to f_2. This confirms the expected agreement.

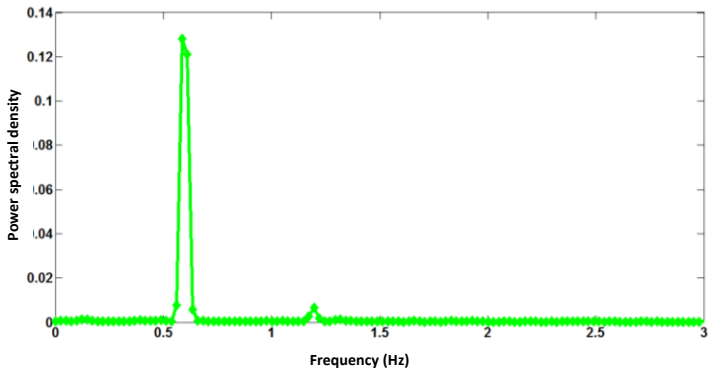

Figure 7: Power spectrum of the transverse velocity signal measured in the mixing layer

4 Step 4: Robustness of seiching: slight geometry modification

The aim of the present section (step 4) is to measure the influence of a slight modification of the cavity width W on the cavity oscillation: the cavity width is increased to W'=0.35m, all other parameters remaining fixed. The consequences in terms of mixing-layer oscillations compared to the square cavity configuration are that:

- the frequency peak near f_{1ADV} (~0.6Hz) almost completely disappeared (see Fig. 8a) so as the corresponding transverse standing wave 3 in the cavity (not shown here).
- the velocity frequency peak f_{2ADV} remains high (see Fig. 8a), so as the corresponding transverse standing wave 1 in the cavity (not shown here).
- a new peak at frequency f_{3ADV}=2.59Hz appears, which equals to the natural frequency f_{nat}=2.56Hz of the cavity corresponding to the length L=0.3m and n=2. This new standing wave is thus binodal and occurs along the same direction as the uninodal one of frequency f_2 (see Fig. 8b, c).

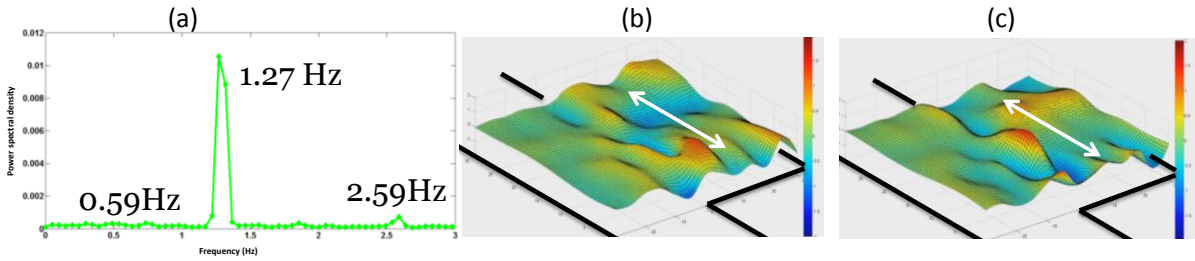

Figure 8: Increased width cavity: transverse velocity power spectrum measured in the mixing layer (a) and reconstruction of the 2D free-surface for the new frequency f3 during the crest (b) and drought (c) at the reference sensor location.

Conclusions

The seiching phenomenon, *i.e.* sustained oscillations of the free surface, was studied experimentally in a lateral, open-channel cavity with adjustable dimensions. Water surface oscillations were recorded and correlated with velocity measurements in the mixing layer and their corresponding frequency spectra.

- To the authors' knowledge, cavities investigated in the literature have dimensions (w+b) and L that are not multiples of each other. Hence, natural frequencies are different in the streamwise and crosswise directions and seiches form in only one direction. The present study, with a cavity such as (w+b)=2L in steps 1, 2 and 3 proves that seiching can develop simultaneously in streamwise and crosswise directions.
- The use of usual signal processing tools allows isolating the different waves constituting the water body oscillation, which frequencies correspond to the natural frequencies of the cavity
- The robustness of the phenomenon was tested. A modification so small as (w+b)=2.17L makes the crosswise wave disappear. It is replaced by a second streamwise wave, binodal, that adds to the first, uninodal one.

Future work must be devoted to the interaction phenomena observed. First one is the interaction of waves of different frequencies, where the largest amplitude can pass from one wave to another. Second is the feedback phenomenon from the seiche to the mixing layer, where two frequency peaks are clearly visible.

References

Cai W., Brosset M., Mignot E., & Riviere N., 2014. Measurement of mass exchange between a main flow and an adjacent lateral cavity. In *International Conference on Fluvial Hydraulics* (River Flow 2014), Lausanne, Switzerland.

Loucks R.B., & Wallace J.M., 2012. Velocity and velocity gradient based properties of a turbulent plane mixing-layer. *J. of Fluid Mech*. 699, 280–319.

Refmar (Réseaux de référence des observations marégraphiques). Seiche. 2014. *Available at*: http://refmar.shom.fr/fr/applications_maregraphiques/etudes-meteo-oceaniques/seiche

Riviere N., Garcia M., Mignot E., & Travin G., 2010. Characteristics of the recirculation cell pattern in a lateral cavity. In *International Conference on Fluvial Hydraulics* (River Flow 2010), Braunschweig, Germany, p. 673 .

Sanjou M., Akimoto T., & Okamoto T., 2012. Three-dimensional turbulence structure of rectangular side-cavity zone in open channel streams. *Int. J. River Basin Management* 10 (4), 293–305.

Sanjou M., & Nezu I., 2013 Hydrodynamic characteristics and related mass-transfer properties in open-channel flows with rectangular embayment zone. *Environ Fluid Mech*. 13 (6), 527–555.

Sorensen R., & Thompson E., 2006. Harbor hydrodynamics. Chapter 7.

Tuna B.A., Tinar E., & Rockwell, D., 2013. Shallow flow past a cavity: globally coupled oscillations as a function of depth. *Exp. in Fluids* 54, 1586.

Wüest A., & Farmer D.M., 2003. Seiches. *McGraw-Hill encyclopedia of science & technology*.